Clinical Oral Investigations
https://doi.org/10.1007/s00784-020-03497-w

ORIGINAL ARTICLE

Diagnostic efficacy of CBCT, MRI, and CBCT-MRI fused images in distinguishing articular disc calcification from loose body of temporomandibular joint

Ying-hui Wang[1] · Gang Li[1] · Ruo-han Ma[1] · Yan-ping Zhao[1,2] · Hao Zhang[2] · Juan-hong Meng[2] · Chuang-chuang Mu[1] · Chong-ke Sun[1] · Xu-chen Ma[1,2]

Received: 5 May 2020 / Accepted: 3 August 2020

Abstract

Objectives To evaluate the diagnostic efficacy of CBCT-MRI fused images for articular disc calcification of temporomandibular joint (TMJ).

Materials and methods Twenty patients (24 TMJs) whose image examinations showed dense bodies in the TMJ space were included in the study. The locations of dense bodies evaluated by the three experts were used as a reference standard. Three oral and maxillofacial radiology residents evaluated whether the dense bodies were disc calcification or not, with a five-point scale for four sets of images (CBCT alone, MRI alone, both CBCT and MRI observed at a time, and CBCT-MRI fused images) randomly and independently. Each set of images was observed at least 1 week apart. A second evaluation was performed after 4 weeks. Intraclass correlation coefficients were calculated to assess the intra- and inter-observer agreement. The areas under the ROC curves (AUCs) were compared between the four image sets using Z test.

Results Ten cases were determined as articular disc calcifications, and fourteen cases were recognized as loose bodies in the TMJ spaces. The average AUC index for the CBCT-MRI fused images was 0.95 and significantly higher than the other sets ($p < 0.01$). The intra- and inter-observer agreement in the CBCT-MRI fused images (0.90–0.91, 0.93) was excellent and higher than those in the other images.

Conclusions CBCT-MRI fused images can significantly improve the observers' reliability and accuracy in determining articular disc calcification of the TMJ.

Clinical relevance The multimodality image fusion is feasible in detecting articular disc calcification of the TMJ which are hard to define by CBCT or MRI alone. It can be utilized especially for inexperienced residents to shorten the learning curve and improve diagnostic accuracy.

Keywords Temporomandibular joint disc · Calcification · Joint loose bodies · Diagnosis · Cone beam computed tomography · Magnetic resonance imaging

✉ Gang Li
kqgang@bjmu.edu.cn

Ying-hui Wang
1811110489@pku.edu.cn

Ruo-han Ma
525943920@qq.com

Yan-ping Zhao
Kqzhao@bjmu.edu.cn

Hao Zhang
zhanghao@hsc.pku.edu.cn

Juan-hong Meng
jhmeng@263.net

Chuang-chuang Mu
muchuangchuang@pku.edu.cn

Chong-ke Sun
771946970@qq.com

Xu-chen Ma
kqxcma@bjmu.edu.cn

[1] Department of Oral and Maxillofacial Radiology, Peking University School and Hospital of Stomatology, #22 Zhongguancun Nandajie, Haidian District, Beijing 100081, China

[2] Center for Temporomandibular Disorders and Orofacial Pain, Peking University School and Hospital of Stomatology, #22 Zhongguancun Nandajie, Haidian District, Beijing 100081, China

Published online: 12 August 2020

Introduction

Image examination constitutes an indispensable element for the diagnosis of temporomandibular joint (TMJ) diseases in nowadays clinical work. In recent years, cone beam computed tomography (CBCT) which has a high spatial resolution has become a dose- and cost-effective alternative to helical CT for the diagnosis of osseous abnormalities of TMJ [1]. Meanwhile, due to the low-density distinguishable ability of CBCT, its detection on soft tissues is poor. Thus, magnetic resonance imaging (MRI) is still used to assess disc position, disc form, presence/absence of fluid within the joint space (joint effusion), marrow signal of the condyle, and pannus formation (in the case of inflammatory arthritis) [2–4]. However, owing to different limitations, neither CBCT nor MRI provides enough information for TMJ region which includes both hard and soft surrounding tissues. In certain clinical cases, it is useful to be able to visualize both soft and hard tissues simultaneously.

In the 1990s, a technique called multimodal medical image fusion was introduced. This technique refers to the intelligent synthesis of medical images from multiple modalities, making full use of the complementarity from different types of medical images to obtain a more reliable and accurate medical image for clinical diagnosis and treatment [5]. CT-MRI fusion technique has been widely applied in clinical research on spinal and brain diseases, chronic otitis media, nasopharyngeal carcinoma (NPC), etc. [6–10]. In oral and maxillofacial region, CT/CBCT-MRI fused images are used for the diagnosis of jaw tumors and the treatment plans for orthodontic and orthognathic patients [11–13]. Different techniques have been explored to fuse MRI and CT/CBCT images of the TMJs [14–17]. Al-Saleh et al. demonstrate that the CBCT-MRI fused image not only improves the intra- and inter-examiner consistency in the evaluation of internal derangement of TMJ but also improves the novice examiners' assessment accuracy of disc positions [18, 19]. Ma et al. verify that the CT/CBCT and MRI images can be fused to aid detection of TMJ anatomical structures and related lesions [20].

Radiological dense bodies within the joint space are either disc calcifications or loose bodies which might occur in many diseases, such as synovial chondromatosis (SC), osteoarthritis, intracapsular fractures, osteochondrosis dissecans, calcium pyrophosphate dihydrate (CPPD) crystal deposition disease, tumoral calcinosis (TC), juvenile idiopathic arthritis, etc. [21–23]. Loose bodies within the temporomandibular joint space might be associated with degenerative arthritis, accompanied by condylar bone erosion [22]. The center of the loose bodies would be composed of dead cancellous bone which represents a detached osteophyte or fibrillated cartilage [21].

Disc calcification of temporomandibular joint is an uncommon lesion. It is a type of dystrophic calcification [24]. Calcifications are more frequently recognized posteriorly than anteriorly and related to disc perforation. The calcification itself may not produce obvious discomfort and can be found by accident. The calcification of articular disc may be stick type, mass type, or punctate type in radiologic findings [23–27]. Clinically, differential diagnosis between disc calcification and loose body of TMJ is important since the former does not need further treatment.

Cases with the application of CBCT and MRI fused image to the diagnosis of TMJ articular disc calcification have been positively reported [20, 26]; however, studies with more cases and identification of observer's reliability are still needed. Therefore, the purpose of this study was first to evaluate the diagnostic efficacy of fused CBCT and MRI images for detection of articular disc calcification of temporomandibular joint and then compare it with CBCT and MRI image observations alone or a combined observation of both CBCT and MRI images at a time, just like in an ordinary clinical situation.

Methods and materials

Subjects

With a preliminary study, the detection rate of dense body in the temporomandibular joint space was 0.9%. Assuming that both sensitivity and specificity for the detection of dense body in the temporomandibular joint space were 0.8, 20 positive cases were needed.

CBCT images taken from the patients who firstly visited the Center for Temporomandibular Disorders and Orofacial Pain in Peking University School and Hospital of Stomatology from 2015 to 2019 were reviewed. The inclusion criteria were as follows: (1) CBCT image showed dense body (one or more) in the TMJ space; (2) for diagnostic purpose, the same patient was captured with MRI scan; and (3) the age of the patient was over 18 years old. The exclusion criteria were as follows: (1) CBCT image showed definite TMJ fracture, ankylosis, or tumor; (2) the patient did not take an MRI examination immediately after the CBCT examination; (3) patients had a clear history of trauma, swelling, infection, or intolerable severe pain in the temporomandibular joint area; and (4) the age of the patient was under 18 years old.

All the image data sets obtained from CBCT and MRI were exported as DICOM (digital imaging and communications in medicine) format.

CBCT and MRI image acquisition

Each CBCT scan was acquired in a 360° rotation for the patient whose Frankfort plane is parallel to the floor in a sitting position. The thyroid collar was used. Images of each TMJ were obtained in the maximal intercuspation. Scans were

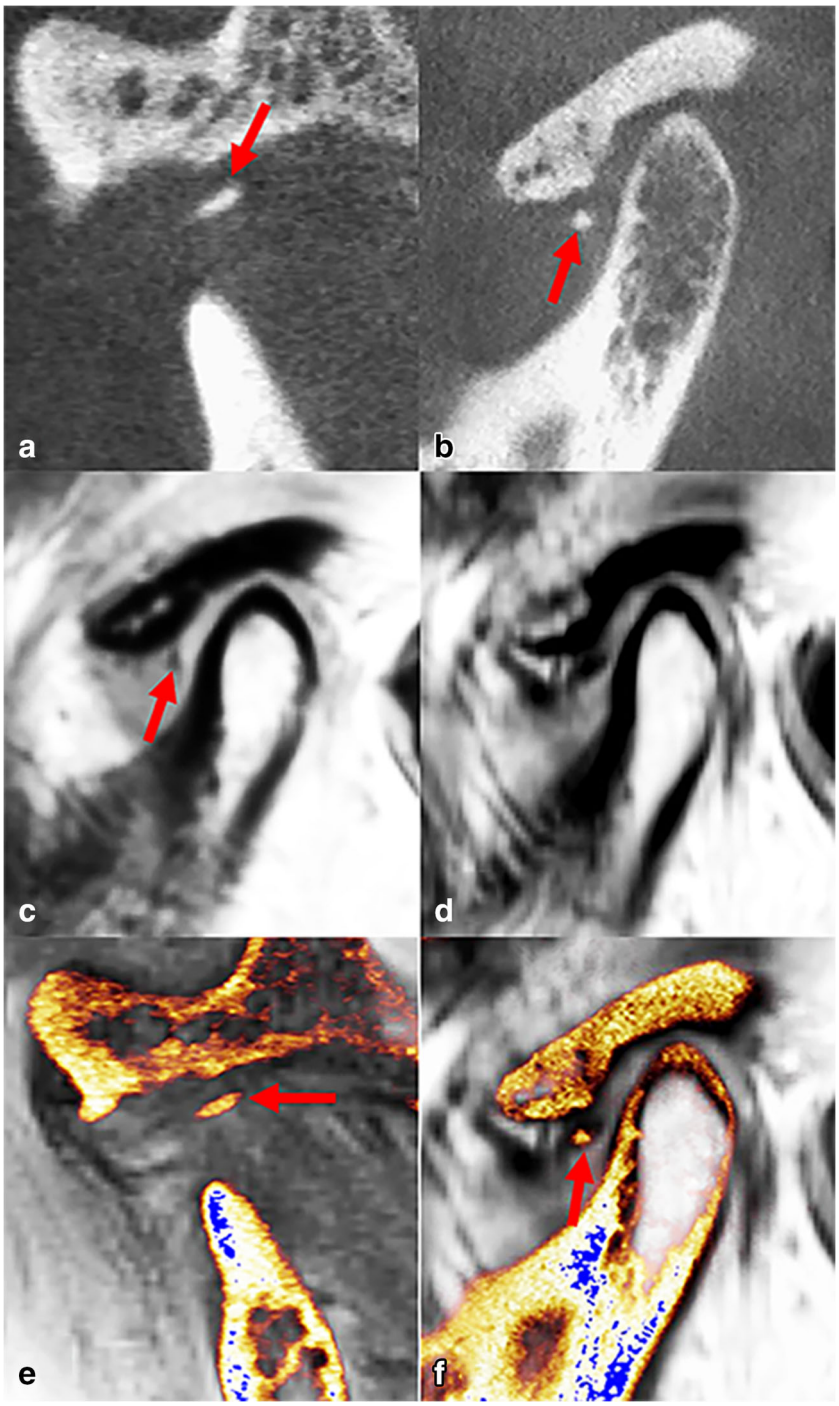

Fig. 1 Example images for the articular disc calcification of TMJ (arrows). Oblique coronal (**a**) and sagittal (**b**) view of the CBCT images. Oblique sagittal view of the MRI image in T_1WI (**c**) and in PDWI (**d**). Oblique coronal view of the CBCT-MRI (T_2WI) fused image (**e**). Oblique sagittal view of the CBCT-MRI (PDWI) fused image (**f**). CBCT, cone beam CT; PDWI, proton density-weighted imaging; T_1WI, T_1-weighted imaging; T_2WI, T_2-weighted imaging

performed using 3D Accuitomo 170 (J Morita Mfg., Corp., Kyoto, Japan) at a field of view (FOV) of 6 cm in diameter and 6 cm in height. The exposure parameters were as follows: scanning time of 17.5 seconds, tube current of 4–5 mA, tube potential of 80–90 kVp, and a voxel size of 0.125 mm according to patients' size. The scan included one side of the TMJs and part of the mandible.

MRI of the TMJs was performed in the supine position without sedation or intravenous contrast administration using a 3.0 T magnet (Siemens Trio Tim, Germany) with a 32-channel surface receiver coil. Patients were scanned in axial, oblique sagittal positions that were perpendicular to the long axis of the condyle and oblique coronal positions that were parallel to the long axis of the condyle. Images were obtained in both maximal intercuspation and maximal voluntary interincisal mouth opening position.

Proton density-weighted images (PDWI) were obtained with a FOV of 14 × 14 cm, slice thickness of 3 mm (11 slices

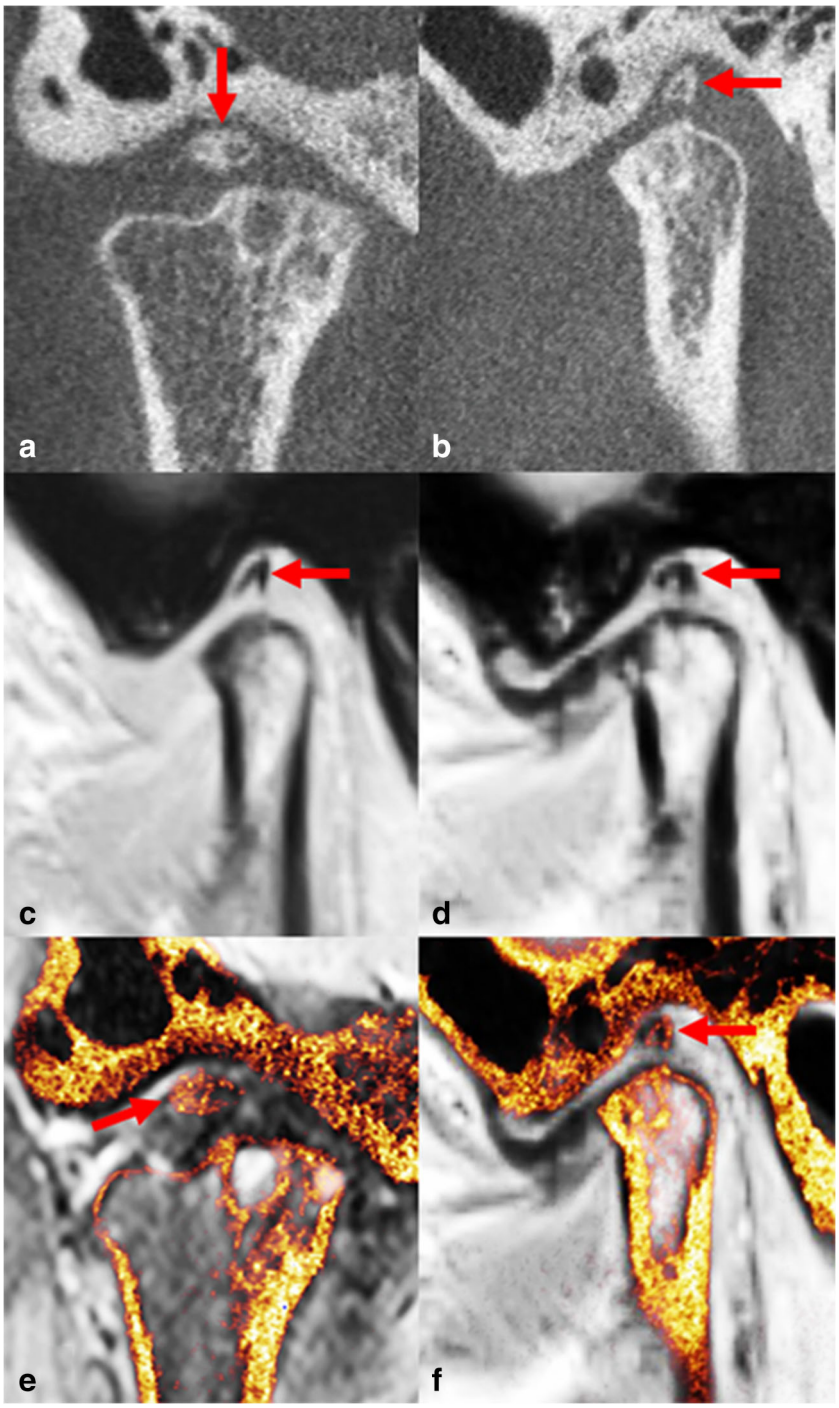

Fig. 2 Example images for the loose body in the TMJ space (arrows). Oblique coronal (**a**) and sagittal (**b**) view of the CBCT images. Oblique sagittal view of the MRI image in T_1WI (**c**) and in PDWI (**d**). Oblique coronal view of the CBCT-MRI (T_2WI) fused image (**e**). Oblique sagittal view of the CBCT-MRI (PDWI) fused image (**f**). CBCT, cone beam CT; PDWI, proton density-weighted imaging; T_1WI, T_1-weighted imaging; T_2WI, T_2-weighted imaging

per TMJ), interslice gap spacing of 0.3 mm, echo time (TE) of 20 ms, repetition time (TR) of 4120 ms, and voxel size of 0.5469 × 0.5469 mm. The difference between T_2-weighted images (T_2WI) and the PDWI was the echo time, which was 99 ms for T_2WI. T_1-weighted images (T_1WI) were obtained with repetition time of 250 ms, echo time of 2.7 ms, and voxel size of 0.4375 × 0. 4375 mm; the rest settings were the same as those in the PDWI acquisition. PDWI and T_1WI were dedicated to the bilateral closed-mouth oblique sagittal sections. T_2WI was used for the bilateral closed-mouth axial, oblique sagittal, oblique coronal positions and bilateral open-mouth oblique sagittal positions.

Imaging registration and fusion

Image fusion of CBCT and MRI images was carried out using the Amira visual software (version 5.4.3, ThermoFisher Scientific Inc.), and the registered process was conducted in

Table 1 Intra-observer consistency for each of the four image sets (ICC [95% CI])

	Observer 1	Observer 2	Observer 3
CBCT	0.82 (0.63, 0.92)	0.80 (0.59, 0.91)	0.81 (0.60, 0.92)
MRI	0.70 (0.43, 0.86)	0.62 (0.29, 0.81)	0.60 (0.27, 0.80)
CBCT+MRI	0.79 (0.57, 0.90)	0.76 (0.52, 0.89)	0.84 (0.65, 0.93)
CBCT-MRI	0.91 (0.80, 0.96)	0.91 (0.80, 0.96)	0.90 (0.78, 0.96)

ICC values [28], agreement was rated as "poor" (< 0.50), "moderate" (0.50–0.75), "good" (0.75–0.90), and "excellent" (> 0.90). CBCT+MRI, a combined observation of CBCT and MRI; CBCT-MRI, fused image of CBCT and MRI

the multiplanar viewer module. On account of the differences in the patient positioning and different size of the acquisition matrix in both image sets, rigid transform model and the similarity metric of normalization mutual information were used for registration in the present study so that the CBCT images would coincide with MRI images. The detailed information could be found in the previous study [20]. The CBCT-MRI fused images were displayed in a color-coded fashion. The overlapped structures from MRI appeared in gray scale, and structures from CBCT appeared in luminous yellow color.

Image evaluation

One specialist with an experience of over 25 years in oral and maxillofacial radiology and two certified specialists with an experience of over 30 years in oral and maxillofacial surgery (mainly for diagnosis and conservative treatment of temporomandibular joint disease) acted as expert panel. The specialists individually determined whether the dense body in the TMJ space was an articular disc calcification or just loose body in the images on the basis of the patient information including patient history, clinical examination, and all the examining images (CBCT images, MRI images, and CBCT-MRI fused images). In case that the determination is not the same, a consensus was reached in the end. The location of dense body evaluated by the expert panel was used as a reference standard.

Three oral and maxillofacial radiology residents with at least 3 years of experience in CBCT image interpretation acted as observers. Before evaluation, the observers were calibrated with an additional session of images in which the disc calcification, the theory of the image fusion technique, and the interpretation of the fused image were explained.

Three residents evaluated the location of dense bodies in the 24 TMJs in four sets of images (CBCT images alone, MRI images alone, both MRI and CBCT images observed at a time, and CBCT-MRI fused images) randomly and independently. Each set of the images was observed at least 1 week apart. The observers assessed the images with five diagnostic alternatives: 1, definitely not articular disc calcification; 2, probably not articular disc calcification; 3, questionable; 4, probably articular disc calcification; and 5, definitely articular disc calcification.

All images were randomly displayed on a Nio Color 5.8 MP (MDNC-6121) display (Barco, Beijing, China) in a quiet room. The orientation, color gradient, brightness, contrast, and magnification of the image could be modified and adjusted to reach the best display. There is no time limit for evaluation. A second evaluation was performed under the same conditions after 4 weeks by the same observers to assess the intra-observer agreement.

Statistical analysis

Data analysis was conducted using the SPSS software, version 20.0 (SPSS Inc., Chicago, IL). A p value of 0.05 or less was considered significant. Intraclass correlation coefficients (ICCs) were calculated to assess the intra- and inter-observer agreement. ICC estimates and their 95% confident intervals were calculated based on a single-rating (intra-agreement)/mean-rating (inter-agreement), absolute-agreement, 2-way mixed-effects model. The ICC values were interpreted as poor (< 0.50), moderate (0.50–0.75), good (0.75–0.90), or excellent (> 0.90) [28]. Scores from the three observers were combined to generate a pooled ROC curve for each image set. The areas under the ROC curves (AUCs) were compared between the four sets using Z test for two independent ROC curves through the MedCalc Statistical Software version 15.2.2 (MedCalc Software bvba, Ostend, Belgium; 2015).

Table 2 Inter-observer agreement for each of the four image sets

	ICC	95% CI
CBCT	0.90	0.79–0.95
MRI	0.74	0.49–0.88
CBCT+MRI	0.81	0.62–0.91
CBCT-MRI	0.93	0.86–0.97

ICC values [28], agreement was rated as "poor" (< 0.50), "moderate" (0.50–0.75), "good" (0.75–0.90), and "excellent" (> 0.90). CBCT+MRI, a combined observation of CBCT and MRI; CBCT-MRI, fused image of CBCT and MRI

Results

Twenty patients with 24 TMJs were included in this retrospective study with a gender predilection of 1:19 (male: 1, female: 19). Their age ranged from 20 to 72 years, with a mean age of 49.57 ± 16.75 years. Altogether, four cases were affected in bilateral, and ten cases were on the right

Table 3 Area under the receiver operating characteristic curve (AUC) for the four image sets

	Observer 1	Observer 2	Observer 3	Mean	SD	Total (the three observers combined, 95% CI)
CBCT	0.84	0.76	0.82	0.81	0.05	0.81 (0.70, 0.89)
MRI	0.73	0.66	0.84	0.74	0.09	0.77 (0.65, 0.86)
CBCT+MRI	0.75	0.80	0.86	0.80	0.06	0.79 (0.68, 0.88)
CBCT-MRI	0.90	0.95	0.99	0.95	0.04	0.95 (0.87, 0.99)

CBCT+MRI, a combined observation of CBCT and MRI; CBCT-MRI, fused image of CBCT and MRI

side and six cases on the left. Five cases were asymptomatic, just for routine examination before prosthodontics and orthodontics. Four cases had noise, pain, and mouth-open limitation (less than 35 mm) simultaneously, and one of them had involuntary twitch of masticatory muscles. Five cases had noise and pain without mouth-open limitation. Three cases only had noise, two cases only had pain, and one case only had mouth-open limitation. They suffered for 3 months to several years. Three of the symptomatic patients underwent operation, and the remainder received conservative treatment.

Ten cases were determined as articular disc calcifications, and fourteen cases were recognized as loose bodies in the temporomandibular joint spaces by the expert panel. Among all, three cases of loose bodies were pathologically confirmed to be synovial chondromatosis, which were consistent with the panel's diagnosis. Articular disc calcifications were of strip type or mass type in the CBCT images. Three out of ten cases showed condylar osteophyte and 1/10 showed wear of condylar bone. As for MRI, two cases indicated anterior disc displacement without reduction, and five were with reduction. The low signal in TMJ space in the T_1WI suggested dense body. It is difficult to distinguish dense bodies from articular discs in PDWI and T_2WI since they were both low-signal areas. In the fused image of CBCT and MRI, however, we could see the calcification overlapping with the articular disc distinctly (Fig. 1), while the loose body was shown separately from the articular disc (Fig. 2).

The intra- and inter-observer agreement in the detection of four image sets is shown in Tables 1 and 2. Both of the ICC values for the intra- and inter-observer agreement were above or equal to 0.90 for the fused CBCT-MRI image set.

The values for AUC from each observer for the four image sets are presented in Table 3. The average value of AUC for the fused image sets of CBCT and MRI was 0.95, which is larger than the values of AUC from the other three image sets. Receiver operating characteristic curves (ROC) from the pooled data of the three observers are shown in Fig. 3. The area under the ROC curve for the CBCT-MRI fused images were higher than those for the other image sets. In addition, there were statistically significant differences between the AUCs of CBCT-MRI fused images and the others, and no significant differences were found between the other three image sets (Table 4).

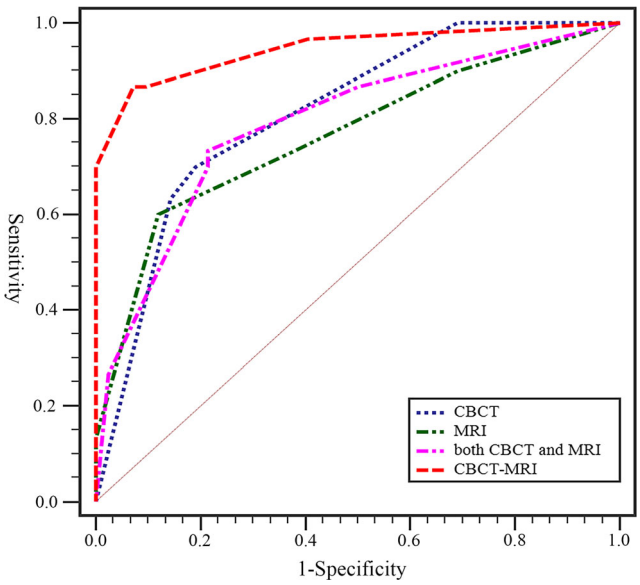

Fig. 3 Receiver operating characteristic curves for the four image sets from pooled data

Discussion

In the present study, the estimated diagnostic accuracy of disc calcification, which was represented by the area under the

Table 4 *p* values when comparing AUC of each image set

	CBCT-MRI	CBCT+MRI	MRI
CBCT	0.00*	0.73	0.52
MRI	0.00*	0.55	–
CBCT+MRI	0.00*	–	–

*Significant difference between the CBCT-MRI fused images and others for AUC. CBCT+MRI, a combined observation of CBCT and MRI; CBCT-MRI, fused image of CBCT and MRI

ROC curve (AUC), was significantly higher for the CBCT-MRI fused images than for the other three observed images. This indicates that fused images from CBCT and MRI are favorable in detecting disc calcification of TMJ. This is further confirmed by the excellent intra-and inter-observer consistency which is indicated by the ICC values. The ICC value for the inter-observer consistence was 0.93, and for the intra-observer consistence, the ICC value was 0.91 for the observer 1, 0.91 for the observer 2, and 0.90 for the observer 3, respectively.

CBCT has a high spatial resolution that can provide high-quality information on the osseous structures of TMJ [29]. It may be easy for junior clinicians to find dense body in the joint space in CBCT images but difficult to extract useful information from MRI images due to the complexity of information containing in the images. One study indicates that even among experienced observers who apply standardized classification criteria, only moderate to substantial observer agreement can be achieved [30]. Thus, juniors must complete learning curve before efficiently reading the images. From the present study, however, the junior observers had a high consistency in diagnosis of TMJ disc calcification with the use of CBCT-MRI fused images. This may be attributed to the fact that the relationship between the TMJ disc and the surrounding skeleton structures, including glenoid fossa, condyle, and dense body, can be finely demonstrated in the CBCT-MRI fused image. This helps the junior observers read the image of TMJ disc calcification in an even better fashion, to improve the diagnostic accuracy. In other words, fused images narrow the disagreement gap within and between each observer so that the subjectivity of diagnosis is minimized. This is in line with the study by Al-Saleh et al. in which the evaluation consistency from two experienced radiologists for the TMJ internal derangement is higher in the registered CBCT-MRI images than in the MRI images alone [18].

The CBCT-MRI fusion technique is innovative and highly useful in the qualification of patients for diagnosis of articular disc calcification of TMJ. Generally, mutual information is used as similarity measure between floating image and reference image to measure the correlation between them. The greater the mutual information, the higher the correlation between the images, the better the fusion effect [31]. This is proved in the previous studies [10, 32, 33] and also identified in the present study.

One limitation of the present study may be the lack of pathological examination as a gold standard for the ROC analysis. However, this is a very common issue for one clinical investigation when surgical treatment is not necessary. In such a situation, a judgment from a panel of experts is usually served as a reference standard. Researchers have found that MRI findings are reliable only when experienced calibrated observers work as a group [34]. Thus, in this study, the evaluation from three experts for the location of dense bodies was used as a reference standard. It is worth notifying that three cases of loose body were pathologically confirmed to be synovial chondromatosis, which were consistent with the panel's diagnosis, certifying that the panel's diagnosis is accurate. Admittedly, errors are still possible, which is unavoidable in this study. Besides, the CBCT-MRI fusion technique is still in the clinical trial stage, and more exploration and research are needed before it can be applied to the clinic as a mature technology.

Conclusion

The multimodality image fusion is a feasible imaging technique for detecting articular disc calcification of the TMJ which are hard to define by CBCT or MRI alone. Using CBCT-MRI fused images, the disc and calcification can be displayed simultaneously, and the diagnostic accuracy is improved considerably.

Funding information The study was supported by the National Natural Science Foundation of China (No. 81671034) and National Key R&D Program of China (No. 2018YFC0807303)

Compliance with Ethical Standards

Conflict of Interest The authors declare that they have no conflict of interest.

Ethical approval All procedures performed in the study involving human participants were in accordance with the ethical standards of Institutional Review Board of Peking University School and Hospital of Stomatology and with the 1964 Helsinki declaration and its later amendments or comparable ethical standards. The study was approved by the Institutional Review Board of Peking University School and Hospital of Stomatology (PKUSSIRB-202054057).

Informed consent Written informed consent was not required for this study because all the included patients in the present investigation were collected retrospectively. Exemption of informed consent will not affect the rights and health of included patients. The application for free informed consent has been approved by the Institutional Review Board.

References

1. Honda K, Larheim TA, Maruhashi K, Matsumoto K, Iwai K (2006) Osseous abnormalities of the mandibular condyle: diagnostic reliability of cone beam computed tomography compared with helical computed tomography based on an autopsy material. Dentomaxillofac Radiol. 35:152–157. https://doi.org/10.1259/dmfr/15831361
2. Tasaki MM, Westesson PL (1993) Temporomandibular joint: diagnostic accuracy with sagittal and coronal MR imaging. Radiology. 186:723–729. https://doi.org/10.1148/radiology.186.3.8430181
3. Hunter A, Kalathingal S (2013) Diagnostic imaging for temporomandibular disorders and orofacial pain. Dent Clin North Am. 57:405–418. https://doi.org/10.1016/j.cden.2013.04.008
4. Talmaceanu D, Lenghel LM, Bolog N, Hedesiu M, Buduru S, Rotar H, Baciut M et al (2018) Imaging modalities for

temporomandibular joint disorders: an update. Clujul Med 91:280–287. https://doi.org/10.15386/cjmed-970
5. Zhou T, Lu H, Chen Z, Ma J (2013) Research progress of multi-model medical image fusion and recognition (article in Chinese). Sheng Wu Yi Xue Gong Cheng Xue Za Zhi. 30:1117–1122
6. Chen YT, Wang MS (2004) Three-dimensional reconstruction and fusion for multi-modality spinal images. Comput Med Imaging Graph. 28:21–31. https://doi.org/10.1016/j.compmedimag.2003.08.001
7. Biesbroek JM, Kuijf HJ, Weaver NA, Zhao L, Duering M, Meta VCIMC, Biessels GJ (2019) Brain infarct segmentation and registration on MRI or CT for lesion-symptom mapping. J Vis Exp. 151: e59653. https://doi.org/10.3791/59653
8. Veninga T, Huisman H, van der Maazen RW, Huizenga H (2004) Clinical validation of the normalized mutual information method for registration of CT and MR images in radiotherapy of brain tumors. J Appl Clin Med Phys. 5:66–79. https://doi.org/10.1120/jacmp.v5i3.1959
9. Kusak A, Rosiak O, Durko M, Grzelak P, Pietruszewska W (2018) Diagnostic imaging in chronic otitis media: does CT and MRI fusion aid therapeutic decision making? - a pilot study. Otolaryngol Pol. 73:1–5. https://doi.org/10.5604/01.3001.0012.5423
10. Wang X, Li L, Hu C, Qiu J, Xu Z, Feng Y (2009) A comparative study of three CT and MRI registration algorithms in nasopharyngeal carcinoma. J Appl Clin Med Phys. 10:3–10. https://doi.org/10.1120/jacmp.v10i2.2906
11. Plooij JM, Maal TJ, Haers P, Borstlap WA, Kuijpers-Jagtman AM, Berge SJ (2011) Digital three-dimensional image fusion processes for planning and evaluating orthodontics and orthognathic surgery. A systematic review. Int J Oral Maxillofac Surg. 40:341–352. https://doi.org/10.1016/j.ijom.2010.10.013
12. Dai J, Wang X, Dong Y, Yu H, Yang D, Shen G (2012) Two- and three-dimensional models for the visualization of jaw tumors based on CT-MRI image fusion. J Craniofac Surg. 23:502–508. https://doi.org/10.1097/SCS.0b013e31824cd433
13. Tai K, Park JH, Hayashi K, Yanagi Y, Asaumi JI, Iida S, Shin JW (2011) Preliminary study evaluating the accuracy of MRI images on CBCT images in the field of orthodontics. J Clin Pediatr Dent 36:211–218. https://doi.org/10.17796/jcpd.36.2.r7853hp574045414
14. Al-Saleh MA, Jaremko JL, Alsufyani N, Jibri Z, Lai H, Major PW (2015) Assessing the reliability of MRI-CBCT image registration to visualize temporomandibular joints. Dentomaxillofac Radiol. 44: 20140244. https://doi.org/10.1259/dmfr.20140244
15. Al-Saleh MA, Punithakumar K, Jaremko JL, Alsufyani NA, Boulanger P, Major PW (2016) Accuracy of magnetic resonance imaging-cone beam computed tomography rigid registration of the head: an in-vitro study. Oral Surg Oral Med Oral Pathol Oral Radiol. 121:316–321. https://doi.org/10.1016/j.oooo.2015.10.029
16. Lin Y, Liu Y, Wang D, Wang C (2008) Three-dimensional reconstruction of temporomandibular joint with CT and MRI medical image fusion technology (article in Chinese). Hua Xi Kou Qiang Yi Xue Za Zhi. 26:140–143. https://doi.org/10.3321/j.issn:1000-1182.2008.02.008
17. Dai J, Dong Y, Shen SG (2012) Merging the computed tomography and magnetic resonance imaging images for the visualization of temporomandibular joint disk. J Craniofac Surg. 23:e647–e648. https://doi.org/10.1097/SCS.0b013e3182710517
18. Al-Saleh MA, Alsufyani NA, Lagravere M, Nebbe B, Lai H, Jaremko JL, Major PW (2016) MRI alone versus MRI-CBCT registered images to evaluate temporomandibular joint internal derangement. Oral Surg Oral Med Oral Pathol Oral Radiol. 122: 638–645. https://doi.org/10.1016/j.oooo.2016.07.024
19. Al-Saleh MA, Alsufyani NA, Lai H, Lagravere M, Jaremko JL, Major PW (2017) Usefulness of MRI-CBCT image registration in the evaluation of temporomandibular joint internal derangement by novice examiners. Oral Surg Oral Med Oral Pathol Oral Radiol. 123:249–256. https://doi.org/10.1016/j.oooo.2016.10.016
20. Ma RH, Li G, Sun Y, Meng JH, Zhao YP, Zhang H (2019) Application of fused image in detecting abnormalities of temporomandibular joint. Dentomaxillofac Radiol. 48:20180129. https://doi.org/10.1259/dmfr.20180129
21. Blenkinsopp PT (1978) Loose bodies of the temporo-mandibular joint, synovial chondromatosis or osteoarthritis. Br J Oral Surg. 16: 12–20. https://doi.org/10.1016/s0007-117x(78)80050-x
22. Anderson QN, Katzberg RW (1984) Loose bodies of the temporomandibular joint: arthrographic diagnosis. Skeletal Radiol. 11:42–46. https://doi.org/10.1007/bf00361131
23. Koyama J, Ito J, Hayashi T, Kobayashi F (2001) Synovial chondromatosis in the temporomandibular joint complicated by displacement and calcification of the articular disk: report of two cases. AJNR Am J Neuroradiol. 22:1203–1206
24. Wu YT (2005) Clinical and imaging diagnosis of oral and maxillofacial bone diseases. Peking University Medical Press, Beijing
25. Marchetti C, Bernasconi G, Reguzzoni M (1997) Presence of calcified tissue in the human temporomandibular joint disc. Arch Oral Biol. 42:755–760. https://doi.org/10.1016/s0003-9969(97)00033-2
26. Han WH, Meng JH, Li G, Ma XC (2019) Diagnosis of bilateral calcifications of temporomandibular joint disc by image fusion. J Craniofac Surg. 30:e597–e598. https://doi.org/10.1097/SCS.0000000000005628
27. Song J, Long X, Deng M (2018) Temporomandibular joint disc calcification: case report and literature review (article in Chinese). Kou Qiang Ji Bing Fang Zhi. 26:48–51
28. Koo TK, Li MY (2016) A guideline of selecting and reporting intraclass correlation coefficients for reliability research. J Chiropr Med. 15:155–163. https://doi.org/10.1016/j.jcm.2016.02.012
29. Krishnamoorthy B, Mamatha N, Kumar VA (2013) TMJ imaging by CBCT: Current scenario. Ann Maxillofac Surg. 3:80–83. https://doi.org/10.4103/2231-0746.110069
30. Nebbe B, Brooks SL, Hatcher D, Hollender LG, Prasad NG, Major PW (2000) Magnetic resonance imaging of the temporomandibular joint: interobserver agreement in subjective classification of disk status. Oral Surg Oral Med Oral Pathol Oral Radiol Endod. 90: 102–107. https://doi.org/10.1067/moe.2000.106300
31. Li X, Zhang C, Li H, Zang X (2010) Development of Medical Image Registration Technology (article in Chinese). Comput Sci. 37:27–33. https://doi.org/10.3969/j.issn.1002-137X.2010.07.006
32. Ma RH, Li G, Yin S, Sun Y, Li ZL, Ma XC (2019) Quantitative assessment of condyle positional changes before and after orthognathic surgery based on fused 3D images from cone beam computed tomography. Clin Oral Investig. 24:2663–2672. https://doi.org/10.1007/s00784-019-03128-z
33. Al-Saleh MA, Punithakumar K, Lagravere M, Boulanger P, Jaremko JL, Major PW (2017) Three-dimensional assessment of temporomandibular joint using MRI-CBCT image registration. PloS One. 12:e0169555. https://doi.org/10.1371/journal.pone.0169555
34. Widmalm SE, Brooks SL, Sano T, Upton LG, McKay DC (2006) Limitation of the diagnostic value of MR images for diagnosing temporomandibular joint disorders. Dentomaxillofac Radiol. 35: 334–338. https://doi.org/10.1259/dmfr/23427399